

Minimal Surfaces from Monopoles

Anthony Small¹

Mathematics Department

National University of Ireland, Maynooth

Co. Kildare, Ireland.

asmall@maths.may.ie

Abstract.

The geometry of minimal surfaces generated by charge 2 Bogomolny monopoles on \mathbb{R}^3 is described in terms of the moduli space parameter k . We find that the distribution of Gaussian curvature on the surface reflects the monopole structure. This is elucidated by the behaviour of the Gauss maps of the minimal surfaces.

2000 *Mathematics Subject Classification.* Primary 53A10; Secondary 53C07, 81T13

§1. Introduction.

In [5], it was shown that the data comprising a static $SU(2)$ monopole on \mathbb{R}^3 are encoded in its *spectral curve*, an auxiliary algebraic curve in \mathbb{T} , the total space of the holomorphic tangent bundle of \mathbb{P}_1 . \mathbb{T} is viewed as the space of all oriented lines in \mathbb{R}^3 , and the spectral curve parameterises the monopole's *spectral lines*. These lines should be thought of as going through the locations of the monopole particles, [6]. For a monopole of charge ℓ , the spectral curve is an ℓ -fold branched cover of \mathbb{P}_1 , of virtual genus $(\ell - 1)^2$. For further details and background information see [2], [11], [20] and [21].

Recall that \mathbb{T} compactifies, by the addition of a single point at infinity, to a quadric cone $\mathcal{C}(Q)$, with vertex v say, in \mathbb{P}_3 . Classical osculation duality gives a correspondence between full curves on $\mathcal{C}(Q)$, and certain full curves in $\mathbb{P}_3^* = \mathbb{C}^3 \cup v^*$. The latter give null curves in \mathbb{C}^3 , and hence project to (branched) minimal surfaces in \mathbb{R}^3 : in fact all non-planar minimal surfaces in \mathbb{R}^3 arise in this way. This correspondence was discovered by Lie, see [3], [5]. The main features of a minimal surface, i.e. the total Gaussian curvature, end structure, branch points and symmetries may be read off the auxiliary curve in \mathbb{T} , see [16] for further details.

Accordingly, a monopole on \mathbb{R}^3 generates, and is determined by, an auxiliary minimal surface in \mathbb{R}^3 : this was observed in [1] and [5]. (However, the correspondence is not understood directly, but via the spectral curve.) Two simple questions arise:

¹On leave at: Faculty of Mathematics, University of Southampton, Southampton SO17 1BJ, England.

- what do these minimal surfaces look like?
- How does the geometry of the auxiliary surface reflect a monopole's structure?

Unfortunately, for charge $\ell \geq 2$, the surfaces are extremely complicated. However, we show that for $\ell = 2$, the key features are tractible, describe them, and indicate briefly how they relate to the monopole.

Recall that the orbits of the Atiyah-Hitchin manifold \mathcal{M}_2^0 , are parameterised by the elliptic modulus $k \in [0, 1)$, see [2]. For $k \neq 0$, each orbit contains a reduced, centred monopole with elliptic spectral curve S_k , as described in §2. The main technical contribution here, which is given in Theorem 4.7, is the derivation of a set of tractible formulae, involving elliptic functions, for the components of the auxiliary null curves determined by osculation of S_k , $k \in (0, 1)$.

Now, for a generic monopole of charge $\ell \in \mathbb{N}$, the auxiliary minimal surface is complete, finitely branched and of finite total curvature $-4\pi\ell$, ℓ being equal to the degree of the Gauss map of the minimal surface. The global structure of such objects is well understood, largely as a result of the seminal work of Osserman [14], see [13] and [15], for further details. Their geometry is ‘concentrated’ in the sense that, ‘from infinity one sees a finite number of planes passing through the origin’, see [12] for a precise statement.

Observe then that the total Gaussian curvature on the minimal surface equals minus the total energy of the monopole. The results described here show moreover that for $\ell = 2$, the *local* distribution of Gaussian curvature on the minimal surfaces, as k varies, reflects the ‘monopole dynamics’. This is closely related to the behaviour of the area measure induced on the spectral curve by the monopole’s ‘Gauss map’, i.e. the branched covering map $\pi : S_k \rightarrow \mathbb{P}_1$. Thus the energy of the monopole is tied to the twisting of its spectral lines.

For $\ell = 2$, $k \neq 0$, the auxiliary minimal surfaces are two ended Klein bottles, where the ends are perpendicular to the spectral lines through the origin. The geometry of each of these surfaces is organised by the configuration of six branch points in the metric on the surface. These are connected by a ‘pointed star’ on the surface, Γ_{S_k} , formed from the image of four of the quarter-period circles of S_k . The Gaussian curvature localises on parts of this star to a degree that varies with k . In particular, as $k \rightarrow 1$, and the monopoles become well-separated, the Gaussian curvature localises at the two monopole particles. Moreover, in this limit, the normal lines to the minimal surface in the vicinity of the particles become exponentially close, relative to separation distance, to monopole spectral lines. Monopole scattering, cf. [2], is reflected by an exchange of Gaussian curvature in which ‘particles of curvature’ become more or less attenuated according to their role in the interaction: the behaviour of the Gauss maps of the minimal surfaces on Γ_{S_k} , as k varies, elucidates this.

The paper is organised as follows. In §2 we briefly review background material

about osculation duality. In §3 we see what can be said about the charge 2 case prior to writing down explicit formulae. §4 contains the main technical results of the paper. These enable us to write down explicit formulae for the minimal surfaces which elucidate a number of subtle features of their geometry. In particular, they furnish a useful formula for the Gauss maps of these surfaces in terms of the moduli parameter k . This allows us to study the area measure induced by the Gauss maps on the spectral curves in the limits $k \rightarrow 0, 1$. These and other issues are explored in §5 – §8.

§2. Osculation duality.

Let $\pi : \mathbb{T} \rightarrow \mathbb{P}_1$ be the projection map. Let ζ be an affine coordinate on \mathbb{P}_1 and (ζ, η) be the coordinates given by $(\zeta, \eta) \rightarrow \eta \frac{d}{d\zeta}$. $H^0(\mathbb{P}_1, \mathcal{O}(\mathbb{T})) \cong \mathbb{C}^3$ and the real structure $\tau : \mathbb{T} \rightarrow \mathbb{T}$, given in local coordinates by $(\zeta, \eta) \rightarrow (-\bar{\zeta}^{-1}, -\bar{\eta}\bar{\zeta}^{-2})$, determines the \mathbb{R}^3 of τ -invariant *real sections* of the form

$$\sigma_{(x_1, x_2, x_3)}(\zeta) = ((x_1 + ix_2) - 2x_3\zeta - (x_1 - ix_2)\zeta^2) \frac{d}{d\zeta}.$$

\mathbb{T} parameterizes the oriented lines in \mathbb{R}^3 and, equivalently, the affine null planes in \mathbb{C}^3 .

Intrinsically, classical osculation duality may be understood in terms of the family of global sections osculating a curve $S \subset \mathbb{T}$; this family determines a null holomorphic curve $\Omega : S^* \rightarrow \mathbb{C}^3 \cong H^0(\mathbb{P}_1, \mathcal{O}(\mathbb{T}))$, where S^* is the desingularization of S , punctured at the finite number of points that correspond to points where S osculates a fibre. By duality, the original curve parameterizes the set of affine null hyperplanes osculating the null curve in \mathbb{C}^3 .

If $S \subset \mathbb{T}$, an ℓ -fold branched covering of \mathbb{P}_1 , $\ell \geq 2$, is an irreducible algebraic curve, then osculation duality determines a (finitely) branched minimal immersion $\phi = \text{Re}(\Omega) : S^* \rightarrow \mathbb{R}^3$. The branched metric, ds^2 , induced on S^* , is complete in the sense that every curve that approaches a puncture has infinite length. (The punctures correspond to the ends of the minimal surface.) However it will in general be (finitely) branched, i.e. have isolated zeros. In summary, cf. [16], the geometry of the minimal surface may be discerned from S as follows:

- the ends of the minimal surface correspond to the points where S osculates a fibre;
- the zeros of the branched metric are caused by hyperosculating sections;
- the Gauss map may be identified with $\pi|_S$, and hence has degree ℓ ;
- the total Gaussian curvature $\iint \mathcal{K} ds^2$ of the induced branched metric equals $-4\pi\ell$;
- if S is τ -invariant then ϕ factors through S/τ ;

- if $G \subset \text{SO}(3)$ is the symmetry group of a regular solid and $\tilde{G} \subset \text{SU}(2)$ the corresponding binary group and S is invariant under \tilde{G} then G is a subgroup of the symmetry group of the corresponding minimal surface.

Remark. Ω induces the branched metric $4ds^2$ on S^* .

The geometric correspondence described above underlies the *Weierstrass formulae in free form*. In ‘global form’, in which S is described by a pair of meromorphic functions on a Riemann surface: $(g, f) : M \rightarrow \mathbb{C}^2$, the coordinate functions of the null curve $\Omega : M^* \rightarrow \mathbb{C}^3$ are given by:

$$\Omega_1 = \frac{1}{2} \left(-\frac{1}{2}(1-g^2) \frac{d^2 f}{dg^2} - g \frac{df}{dg} + f \right) \quad (1)$$

$$\Omega_2 = \frac{i}{2} \left(-\frac{1}{2}(1+g^2) \frac{d^2 f}{dg^2} + g \frac{df}{dg} - f \right) \quad (2)$$

$$\Omega_3 = \frac{1}{2} \left(g \frac{d^2 f}{dg^2} - \frac{df}{dg} \right) \quad (3)$$

where $\frac{df}{dg} = \frac{f'}{g'}$ and $\frac{d^2 f}{dg^2} = \left(\frac{df}{dg} \right)' \frac{1}{g'}$, etc. $\phi = \text{Re}(\Omega)$ describes a branched minimal surface in \mathbb{R}^3 . Note that g may be identified with the classical Gauss map of ϕ .

Remark. These formulae are not canonical: their precise shape is determined by the real structure τ , and thus the choice of \mathbb{R}^3 in $H^0(\mathbb{P}_1, \mathcal{O}(\mathbb{T}))$ made in [5]. They differ slightly from the classical formulae, [3]. (Note however that the formulae given in the appendix of [5] require slight adjustment.)

The following is an immediate consequence of the nature of osculation duality.

Proposition 2.1 *Suppose that $S \subset \mathbb{T}$ is the spectral curve of a monopole and $\Omega : S^* \rightarrow \mathbb{C}^3$, the associated null curve. Then the affine null planes in \mathbb{C}^3 that osculate the null curve intersect \mathbb{R}^3 in the spectral lines of the monopole.*

Remark. This requires clarification for charge 1, since in that case the spectral curve is a section, and osculation of it is degenerate, in the sense that it gives only a point in \mathbb{C}^3 . The affine null planes through a point in \mathbb{C}^3 should be viewed as ‘osculating that point’. Similar remarks apply to any spectral curve which includes a global section as a component.

§3. Osculation of spectral curves of charge 2 monopoles.

In this section we describe the main features of the minimal surfaces generated by osculation of charge 2 monopole spectral curves. At this point we refrain from deriving formulae for the minimal surfaces: these are discussed in the next section.

Hurtubise [8], showed that the spectral curve S , of a centred charge 2 monopole, may by rotation of \mathbb{R}^3 , be brought to the reduced form:

$$\eta^2 = r_1\zeta - r_2\zeta^2 - r_1\zeta^3, \quad r_1, r_2 \in \mathbb{R}, \quad r_1 \geq 0. \quad (4)$$

When $r_1 \neq 0$, the triviality of $L^2|_S$ constrains the real period: $\omega_1 = 2\sqrt{r_1}$. At $r_1 = 0$, S degenerates into the pair of global sections given by $\eta^2 = -\pi^2\zeta^2/4$: this gives the reduced form for an axially symmetric monopole. Observe that if $r_1 \neq 0$, then S is a smooth τ -invariant elliptic curve on \mathbb{T} . τ restricted to S takes the form $\tau(u) = -\bar{u} + \omega_3/2$, and has no fixed points: the associated lattice is rectangular.

When $r_1 \neq 0$, the branch points of S are at 0 , ∞ , $-a$, and a^{-1} , where $-a$ and a^{-1} are the roots of $\zeta^2 - \frac{r_2}{r_1}\zeta - 1 = 0$. These two antipodal pairs give α and β , the spectral lines through 0 , the centre of the monopole. The monopole has a distinguished bisector \underline{e}_1 , of the angle between α and β : this is the monopole's *main axis*. (In the axially symmetric case this is the axis of symmetry.) The second bisector, \underline{e}_2 , is the monopole's *Higgs axis*. The perpendicular through 0 to \underline{e}_1 and \underline{e}_2 , is denoted \underline{e}_3 , and called the *third axis*. Having fixed \underline{e}_1 , \underline{e}_2 and \underline{e}_3 , the monopole is determined by an angle $0 \leq \theta < \pi/2$. ($\theta = 0$, gives a centred axially symmetric monopole.) See [2] for further details.

It is observed in [8] that S has symmetries, permuting the roots of (4): these correspond to the subgroup D of $\text{SO}(3)$, comprising rotations through π about the axes \underline{e}_1 , \underline{e}_2 and \underline{e}_3 in \mathbb{R}^3 . D is of course isomorphic to $\mathbb{Z}_2 \times \mathbb{Z}_2$.

Following [2], let $\tan(2\theta) = \frac{2r_1}{r_2}$. 2θ is the angle between the lines α and β . It is natural and eases calculation to introduce the modulus $k = \sin(\theta)$, together with the complementary modulus $k' = \cos(\theta)$. $\text{SO}(3)$ acts naturally on the moduli space \mathcal{M}_2^0 of centred 2-monopoles. The orbits are parameterized by θ , or equivalently, $k \in [0, 1)$. For $\theta = 0$, the orbit is isomorphic to $\mathbb{R}\mathbb{P}_2$: this parameterizes the centred axially symmetric 2-monopoles. For $\theta \neq 0$, the orbit is isomorphic to $\text{SO}(3)/D$. In [2], it is observed that the triviality of $L^2|_S$ means that (4) may be rewritten:

$$\eta^2 = K(k)^2\zeta(kk'(\zeta^2 - 1) + (k^2 - (k')^2)\zeta), \quad (5)$$

where as usual, $K(k) = \int_0^{\pi/2} \frac{d\psi}{\sqrt{1 - k^2 \sin^2 \psi}}$. Accordingly, emphasising k dependence, from now on we refer to this curve as S_k .

Now, a global section σ_z of \mathbb{T} , corresponding to $z \in \mathbb{C}^3$, osculates S_k at p if and only if $\sigma_{\bar{z}}$ osculates S_k at $\tau(p)$, thus $\Omega(\tau(u)) = \overline{\Omega(u)}$, and hence $\phi(\tau(u)) = \phi(u)$. A cursory inspection of the structure of the Weierstrass formulae for these surfaces shows that $\phi(-u) = -\phi(u)$, (cf. Theorem 4.7). These mean that ϕ enjoys many symmetries on the fundamental period rectangle. In particular observe that ϕ is defined on the doubly punctured Klein bottle $S_k/\tau - \{[0], [\omega_3/2]\}$.

As a curve on $\mathcal{C}(Q)$ in \mathbb{P}_3 , S_k has degree 4. The points of hyperosculation on S_k are the points of order 4 in its group structure: this follows from Abel's theorem. Each of the four branch points of $\pi|_{S_k}$, is a point of hyperosculation since the osculating hyperplane at a branch point b say, lies tangent to $\mathcal{C}(Q)$ along the fibre through b , and thus intersects S_k with multiplicity 4 at b . These give the points of order 2 in the group structure of S_k . They come in two antipodal pairs and correspond to the two ends of the minimal surface in \mathbb{R}^3 . This leaves twelve zeros in the branched metric on S_k^* : these pass to six branch points on $S_k/\tau - \{[0], [\omega_3/2]\}$. Comparing these observations with the properties of osculation duality listed in §2 gives:

Proposition 3.1 (i) *Osculation of the spectral curve S_k of a non-axially symmetric centred 2-monopole gives a branched minimal immersion of the punctured Klein bottle $\phi : S_k/\tau - \{[0], [\omega_3/2]\} \rightarrow \mathbb{R}^3$, with the following properties:*

- (ii) *the total Gaussian curvature of the induced branched metric on S_k^* equals -8π .*
- (iii) *The minimal surface has two ends. These are perpendicular to the two spectral lines through the monopole's centre.*
- (iv) *There are six branch points, (of ramification index 1), on the minimal surface in \mathbb{R}^3 . These are:*

$$\pm\beta_1 = \pm\phi(\omega_1/4), \quad \pm\beta_2 = \pm\phi(\omega_2/4) \quad \text{and} \quad \pm\beta_3 = \pm\phi(\omega_3/4).$$

- (v) *The image of $\phi : S_k/\tau - \{[0], [\omega_3/2]\} \rightarrow \mathbb{R}^3$, is invariant under D .*

Remark. Osculation of the (reduced and centred) axially symmetric 2-monopole spectral curve yields the pair of points $(0, 0, \pm\frac{i\pi}{4})$ in \mathbb{C}^3 . (So the auxiliary 'minimal surface' in this case is the point at the origin.)

Locally, around each of the points of hyperosculation that are not branch points of $\pi|_{S_k}$, S_k may be described by $\eta = a_4\zeta^4 + \mathcal{O}(\zeta^5)$, for some $a_4 \in \mathbb{C}$. Hence at each of the branch points the minimal surface is locally a perturbation of a rescaled associate surface of the minimal surface determined by osculation of $\eta = \zeta^4$. It is easy to see directly from calculation that the latter maps the lines $x = 0$, $y = \frac{1}{\sqrt{3}}x$, and $y = -\frac{1}{\sqrt{3}}x$, to the three rays in the $(x_1, x_2, 0)$ -plane at 120° , where $x = 0$, is mapped 2 : 1 onto $\{(x_1, 0) ; x_1 \leq 0\}$, etc. Each of the 60° sectors in the (x, y) -plane is embedded, along with the image of its reflection through the origin, to a surface bounded by two of the rays, cf. Figure 6 in [13]. This *triple curve intersection structure* at the branch point is stable under higher order perturbations and multiplication by a_4 . (Of course, it 'twists' if $a_4 \notin \mathbb{R}$.) Hence we see six of these triple curve intersection structures at the branch points on the monopole minimal surface.

§4. Formulae for the null curve.

In [8], the following substitutions are introduced for $r_1 \neq 0$:

$$\zeta = \tilde{\zeta} + k_2 \quad \text{and} \quad \eta = k_1 \tilde{\eta},$$

where $k_1 = \frac{1}{2}\sqrt{r_1}$ and $k_2 = r_2/3r_1$. Thus (4) becomes

$$\tilde{\eta}^2 = 4\tilde{\zeta}^3 - g_2\tilde{\zeta} - g_3, \quad (6)$$

where $g_2 = 12k_2^2 + 4$ and $g_3 = 8k_2^3 + 4k_2$.

If $\wp(u)$ is the Weierstrass \wp -function determined by g_2 and g_3 , then the spectral curve S is uniformised by $\zeta = g(u) = \wp(u) + k_2$ and $\eta = f(u) = \frac{\omega_1}{4}\wp'(u)$.

Remark. It should be noted that direct substitution of these into the Weierstrass formulae (1)-(3), yields very complicated expressions. We now outline another approach which results in the relatively simple formulae described in Theorem 4.7 below. First the meaning of the parameter k_2 is clarified:

Proposition 4.1 $k_2 = -e_3$.

Proof. $\wp'(\omega_j/2) = 0$, implies $4e_j^3 - g_2e_j - g_3 = 0$, for $j = 1, 2, 3$, and hence

$$(e_j + k_2)(e_j^2 - k_2e_j - (1 + 2k_2^2)) = 0, \quad \text{for } j = 1, 2, 3.$$

The roots of the quadratic factor are $(k_2 \pm \sqrt{9k_2^2 + 4})/2$. The ordering of the roots follows from the elementary fact that for a rectangular lattice $\wp(u)$ takes real values, and is strictly decreasing as u passes around the rectangle with vertices $0, \omega_1/2, \omega_3/2, \omega_2/2$, and hence $e_1 > e_3 > e_2$, see [4]. It follows that $k_2 = -e_3$. \square

Corollary 4.2 *The half-period values of $\wp(u)$ are given by:*

$$e_1 = \frac{2 - k^2}{3kk'}, \quad e_2 = -\frac{1 + k^2}{3kk'} \quad \text{and} \quad e_3 = \frac{2k^2 - 1}{3kk'}. \quad (7)$$

Proof. From the definitions of θ and k_2 , it follows that $k_2 = \frac{1 - 2k^2}{3kk'}$. The result is immediate. \square

Remarks. (i) A simple calculation shows that

$$g_2 = \frac{4(1 - k^2 + k^4)}{3k^2k'^2} \quad \text{and} \quad g_3 = \frac{4(k^2 - 2)(k^2 + 1)(2k^2 - 1)}{27k^3k'^3}. \quad (8)$$

(ii) The periods of S_k are given by:

$$\omega_1 = 2\sqrt{kk'}K(k) \quad \text{and} \quad \omega_2 = 2i\sqrt{kk'}K'(k), \quad (9)$$

where, as usual, $K'(k) = K(k')$, [2].

Lemma 4.3 For $\wp(u)$, with g_2, g_3 determined by k as above:

$$1 + 2\frac{k'}{k}(\wp(u) - e_3) - (\wp(u) - e_3)^2 = \wp'(u)\sqrt{\wp(2u) - e_1} \quad (10)$$

$$-1 + 2\frac{k}{k'}(\wp(u) - e_3) + (\wp(u) - e_3)^2 = -\wp'(u)\sqrt{\wp(2u) - e_2} \quad (11)$$

$$1 + (\wp(u) - e_3)^2 = -\wp'(u)\sqrt{\wp(2u) - e_3} \quad (12)$$

where, in the first formula, i times the radical is positive at $u = \omega_2/4$, and in the other two, the radical is positive at $u = \omega_1/4$.

Proof. The quarter-period formulae of the Appendix, together with the translation formulae, yield:

$$\begin{aligned} \wp\left(\frac{\omega_1}{4}\right) - e_3 &= \wp\left(\frac{3\omega_1}{4}\right) - e_3 = \frac{1 + k'}{k}, \\ \wp\left(\frac{\omega_1}{4} + \frac{\omega_2}{2}\right) - e_3 &= \wp\left(\frac{3\omega_1}{4} + \frac{\omega_2}{2}\right) - e_3 = \frac{-1 + k'}{k}. \end{aligned}$$

Now observe that $(1 + k')/k, (-1 + k')/k$ are the roots of

$$1 + 2\frac{k'}{k}x - x^2 = 0.$$

It is clear that both sides in (10) have poles of order -4 at 0 , and zeros of order 1 at $\omega_1/4, 3\omega_1/4, \omega_1/4 + \omega_2/2$ and $3\omega_1/4 + \omega_2/2$. The scaling is fixed at $\omega_2/4$, cf. the Appendix. (11) and (12) are proved similiarly. \square

Definition. Let $f_j(u)$ denote the square root of $\wp(u) - e_j$, whose residue at the origin is 1 .

These choices of signs accord with those in Lemma 4.3.

Remark. This notation follows [4].

Lemma 4.4 Substitution of $g(u) = \wp(u) - e_3, f(u) = \frac{\omega_1}{4}\wp'(u)$, into (2) yields:

$$\Omega_2(u) = \frac{i\omega_1}{4} \left\{ \frac{1 + (\wp(u) - e_3)^2}{\wp'(u)} \right\}^3.$$

Proof. First observe that

$$g\frac{df}{dg} - f = \frac{\omega_1}{4} \left\{ \frac{gg'' - (g')^2}{g'} \right\}$$

$$\begin{aligned}
&= \frac{\omega_1}{4\wp'} \left\{ 2\wp^3 - 6e_3\wp^2 + \frac{g_2}{2}\wp + g_3 + e_3\frac{g_2}{2} \right\} \\
&= \frac{\omega_1(1+g^2)g}{2g'},
\end{aligned}$$

since $g_2 = 4(1 + 3e_3^2)$, and $g_3 = -4e_3(1 + 2e_3^2)$.

Now observe that $\frac{d^2f}{dg^2} = \frac{\omega_1}{4} \left\{ \frac{g'''g' - (g'')^2}{(g')^3} \right\}$, and hence

$$\begin{aligned}
\Omega_2 &= \frac{i\omega_1(1+g^2)}{16g'^3} \left\{ 4g(g')^2 - g'''g' + (g'')^2 \right\} \\
&= \frac{i\omega_1(1+g^2)}{16g'^3} \left\{ 4\wp^4 - 16e_3\wp^3 + 2g_2\wp^2 + 4(2g_3 + g_2e_3)\wp + 4e_3g_3 + \frac{g_2^2}{4} \right\} \\
&= \frac{i\omega_1}{4} \left\{ \frac{1+g^2}{g'} \right\}^3,
\end{aligned}$$

again using $g_2 = 4(1 + 3e_3^2)$, and $g_3 = -4e_3(1 + 2e_3^2)$. \square

Lemma 4.5

$$\Omega_2(u) = -i\frac{\omega_1}{4}f_3(2u)^3.$$

Proof. This follows immediately from (12) and 4.4. \square

Lemma 4.6 For $g(u) = \wp(u) - e_3$, and $f(u) = \frac{\omega_1}{4}\wp'(u)$:

$$\frac{d^3f}{dg^3}(u) = -3\omega_1\frac{\wp'(2u)}{\wp'(u)^2}. \quad (13)$$

Proof. Differentiate (2) and the formula of Lemma 4.5 and compare, using (12). \square

With respect to the k -monopole coordinates $(\underline{e}_1, \underline{e}_2, \underline{e}_3)$, the null curve is represented by $\Phi = A_k\Omega$, i.e.

$$\begin{pmatrix} \Phi_1 \\ \Phi_2 \\ \Phi_3 \end{pmatrix} = \begin{pmatrix} -k & 0 & k' \\ k' & 0 & k \\ 0 & 1 & 0 \end{pmatrix} \begin{pmatrix} \Omega_1 \\ \Omega_2 \\ \Omega_3 \end{pmatrix} \quad (14)$$

Theorem 4.7 *Suppose that $k \in (0, 1)$, determines g_2, g_3 , as in (8), and $\wp(u)$ is the associated Weierstrass function. The null curve that is generated by osculation of the spectral curve described implicitly by $g(u) = \wp(u) - e_3$, $f(u) = \frac{\omega_1}{4}\wp'(u)$, has components with respect to k -monopole coordinates given by:*

$$\Phi_1(u) = -k\frac{\omega_1}{4}f_1(2u)^3 \quad (15)$$

$$\Phi_2(u) = k'\frac{\omega_1}{4}f_2(2u)^3 \quad (16)$$

$$\Phi_3(u) = -i\frac{\omega_1}{4}f_3(2u)^3 \quad (17)$$

Proof. The formula for $\Phi_3(u)$ is equivalent to that of Lemma 4.5. Differentiating with respect to u :

$$\begin{aligned} \Phi_1'(u) &= g'(u)\frac{d\Phi_1}{dg}(u) \\ &= \frac{k}{4}g'(u)\frac{d^3f}{dg^3}(u)(1-g(u)^2) + 2\frac{k'}{k}g(u) \\ &= -\frac{3}{4}k\omega_1\wp'(2u)f_1(2u) \end{aligned}$$

where the last equality follows from (10), together with Lemma 4.6. Therefore

$$\Phi_1(u) = -k\frac{\omega_1}{4}f_1(2u)^3 + \Phi_1\left(\frac{\omega_1}{4}\right).$$

Now note that it follows from the quarter-period formulae (of the Appendix) that $\Phi_1(\omega_1/4) = 0$.

Similarly,

$$\begin{aligned} \Phi_2'(u) &= g'(u)\frac{d\Phi_2}{dg}(u) \\ &= \frac{k'}{4}g'(u)\frac{d^3f}{dg^3}(u)(-1+g(u)^2) + 2\frac{k}{k'}g(u) \\ &= \frac{3}{4}k'\omega_1\wp'(2u)f_2(2u) \end{aligned}$$

where the last equality follows from (11), together with Lemma 4.6. Therefore

$$\Phi_2(u) = k'\frac{\omega_1}{4}f_2(2u)^3 + \Phi_2\left(\frac{\omega_2}{4}\right).$$

Finally note that it follows from the quarter-period formulae (of the Appendix) that $\Phi_2(\omega_2/4) = 0$. \square

Remark. The nullity of Φ is a special case of the quadratic identity

$$(e_2 - e_3)f_1^2(z) + (e_3 - e_1)f_2^2(z) + (e_1 - e_2)f_3^2(z) = 0.$$

For a normal rectangular lattice this reduces to the following identity between Jacobi functions: $-k^2cs^2(z) - k'^2ns^2(z) + ds^2(z) = 0$. Cf. §4 of [4].

Corollary 4.8 *The branched metric induced on the spectral curve by ϕ has the form:*

$$ds^2(u) = \frac{9}{32}|\wp'(2u)|^2\{k^2|\wp(2u) - e_1| + k'^2|\wp(2u) - e_2| + |\wp(2u) - e_3|\}|du|^2.$$

Remark. Observe that this displays the branching and end structure at the quarter-period points described in §3.

§5. The locations of the branch points.

The following can be derived from Theorem 4.7, (or directly from quarter-period formulae). They are written w.r.t. k -monopole coordinates.

Proposition 5.1

$$\Phi\left(\frac{\omega_1}{4}\right) = \frac{K(k)}{2k}(0, 1, -ik'^2) \quad (18)$$

$$\Phi\left(\frac{\omega_2}{4}\right) = \frac{K(k)}{2k'}(-i, 0, k^2) \quad (19)$$

$$\Phi\left(\frac{\omega_3}{4}\right) = \frac{K(k)}{2}(-ik'^2, k^2, 0) \quad (20)$$

Corollary 5.2 *Projecting to \mathbb{R}^3 gives:*

$$\beta_1 = \frac{K(k)}{2k}(0, 1, 0) \quad (21)$$

$$\beta_2 = \frac{k^2K(k)}{2k'}(0, 0, 1) \quad (22)$$

$$\beta_3 = \frac{k^2K(k)}{2}(0, 1, 0) \quad (23)$$

Remark. Observe that the positions of the branch points are tied to the moduli space parameter k as above, through the non-singularity constraint $L^2|_{S_k} = \mathcal{O}_{S_k}$. There are a number of interesting consequences which we list in the following corollary. First note the following

Definition. For values of k close to 1, by *separation distance* we mean $K(k)$.

Corollary 5.3 (a) *The branch points $\pm\beta_1, \pm\beta_3$, lie on the Higgs axis, \underline{e}_2 .*

(b) *In the ‘widely separated limit’, $k \rightarrow 1$:*

- $\pm\beta_1, \pm\beta_3 \rightarrow \pm \frac{K(k)}{2}(0, 1, 0)$, respectively.

Thus, these pairs of branch points approach the ‘star centres’ exponentially fast relative to the separation distance.

- $\pm\beta_2 \rightarrow \pm\infty$ along \underline{e}_3 , exponentially fast relative to separation distance.

(c) *As $k \rightarrow 0$, and the monopoles approach the axially symmetric solution:*

- $\pm\beta_2, \pm\beta_3 \rightarrow 0$.
- *As $k \rightarrow 0$, $\pm\beta_1$ approach the origin (with $\pm\beta_3$, respectively,) but ‘turn around’, at k_0 , such that $k_0 dK/dk(k_0) = K(k_0)$, and go back out to $\pm\infty$, respectively, along the Higgs axis.*

Remark. $k_0 < 1/\sqrt{2}$, the value that gives the square lattice.

Definition. We call $\pm\beta_1, \pm\beta_3$, the *Higgs branch points*.

Remark. It is instructive to take note of the asymptotic behaviour of the imaginary components at the branch points.

§6. Curves of symmetry of $\phi = \text{Re}(\Phi)$.

Definition.

(i) $V_a := \{a\omega_1 + iy ; 0 \leq y < |\omega_2|\}$.

(ii) $H_a := \{x + a\omega_2 ; 0 \leq x < |\omega_1|\}$.

We study $\Gamma_{S_k} = \phi(H_{\frac{1}{4}} \cup V_{\frac{1}{4}} \cup V_{\frac{3}{4}})$: this is a graph on the minimal surface which connects the six branch points.

Definition. Write $V_{\frac{1}{4}} = V_1 \cup V_2 \cup V_3 \cup V_4$ where $V_j := \{\frac{\omega_1}{4} + iy ; (j-1)\frac{|\omega_2|}{4} \leq y \leq j\frac{|\omega_2|}{4}\}$, $j = 1, 2, 3, 4$.

Proposition 6.1 *The branched minimal immersion ϕ maps $V_{\frac{1}{4}} \cup V_{\frac{3}{4}}$ to the Higgs axis so that: (i) $\phi|_{V_3} = \phi|_{V_1}$ and $\phi|_{V_4} = \phi|_{V_2}$. (ii) ϕ maps V_1 monotonically from β_1 to β_3 .*

(iii) ϕ maps V_2 monotonically from β_3 to β_1 .

(iv) $\phi(\frac{3\omega_1}{4} + iy) = -\phi(\frac{\omega_1}{4} + i(\frac{\omega_2}{2} - y))$.

Proof. (i) follows immediately from $\phi(\tau(u)) = \phi(u)$.

(ii) and (iii): for $u \in V_1 \cup V_2$, $e_3 \leq \wp(2u) \leq e_1$. Hence, for such u , $\phi_1(u) \equiv 0$, and

$\phi_3(u) \equiv 0$. $\phi_2(u)$ monotonically decreases (through real values) from $k'(e_1 - e_2)^{3/2}$ to $k'(e_3 - e_2)^{3/2}$ between $\omega_1/4$ and $\omega_3/4$. It is monotonically increasing between $\omega_3/4$ and $\omega_1/4 + \omega_2/2$.

(iv) follows immediately from $\phi(-\tau(u)) = -\phi(u)$. \square

Proposition 6.2 ϕ maps $H_{\frac{1}{4}}$ monotonically onto the ‘star’ in the $(\underline{e}_2, \underline{e}_3)$ -plane, with vertices $\pm\beta_2, \pm\beta_3$, that is formed when D acts on the concave curve $\phi(\{x + \omega_2/4 ; 0 \leq x \leq \omega_1/4\})$.

Proof. Since $\wp(2u) - e_1 < 0$, for all $u \in H_{\frac{1}{4}}$, it follows from 4.7 that $\phi_1(u) \equiv 0$ on $H_{\frac{1}{4}}$. ϕ_2 is odd at $\omega_2/4$ and $\omega_2/4 + \omega_1/2$, while it is even at $\omega_3/4$ and $\omega_3/4 + \omega_1/2$. On the other hand, ϕ_3 is odd at $\omega_3/4$ and $\omega_3/4 + \omega_1/2$, while it is even at $\omega_2/4$ and $\omega_2/4 + \omega_1/2$. This leads immediately to D -invariance. For $u \in H_{\frac{1}{4}}$, $\wp'(2u)$, $(\wp(2u) - e_2)^{\frac{1}{2}}$ and $(e_3 - \wp(2u))^{\frac{1}{2}}$ are real. Hence, for $u \in \{x + \omega_2/4 ; 0 \leq x \leq \omega_1/4\}$,

$$\frac{d\phi_3}{d\phi_2}(u) = \frac{\operatorname{Re}(\Phi'_3(u))}{\operatorname{Re}(\Phi'_2(u))} = -\frac{1}{k'} \sqrt{\frac{e_3 - \wp(2u)}{\wp(2u) - e_2}}.$$

For such u , $e_3 - \wp(2u)$ monotonically decreases from $e_3 - e_2$ to 0, while $\wp(2u) - e_2$ monotonically increases from 0 to $e_3 - e_2$. Thus observe that the derivative monotonically increases from $-\infty$ to 0 on the curve between β_2 and β_3 . \square

Definition. Write $\Gamma_{S_k} = \Gamma_{\text{Star}}(k) \cup \Gamma_{\text{Higgs}}(k)$, where $\Gamma_{\text{Star}}(k) = \phi(H_{\frac{1}{4}})$.

Note that Γ_{S_k} is D -invariant. Similar arguments give:

Proposition 6.3 (i) ϕ maps V_0 onto the \underline{e}_3 -axis between β_2 and ∞ . Similarly, ϕ maps $V_{\frac{1}{2}}$ onto the \underline{e}_3 -axis between $-\beta_2$ and $-\infty$.

(ii) Near β_2 , $\phi(V_0)$, together with the curves of Γ_{Star} that emanate from β_2 , comprise the triple curve intersection structure at β_2 . The analogue holds at $-\beta_2$.

(iii) The triple curve intersections at $\pm\beta_3$ are induced by Γ_{S_k} .

(iv) ϕ maps H_0 between 0 and $\omega_1/2$, to two arms of the triple curve intersections at β_1 . (The third arm is $\phi(V_{\frac{1}{4}})$.) These two arms emanating from β_1 lie in the $(\underline{e}_1, \underline{e}_2)$ -plane and are concave down. The analogue holds at $-\beta_1$.

§7. Spectral lines near $\Gamma_{\text{Higgs}}(k)$, as $k \rightarrow 1$.

Asymptotically, as $k \rightarrow 1$, $K(k) \sim -\log k'$. Thus observe from (5), that as $k \rightarrow 1$, the configuration of spectral lines approximates the two stars on the Higgs axis through the points at distance $K(k)/2$ from the origin, see [2]. In 5.2, we saw that $\Gamma_{\text{Higgs}}(k)$ shrinks to these points as $k \rightarrow 1$. Here we observe that in this limit the stars approximate the normal lines to the minimal surface in the vicinity of $\Gamma_{\text{Higgs}}(k)$.

The branch points on the null curves in \mathbb{C}^3 which project to the Higgs branch points approach exponentially close to \mathbb{R}^3 , relative to separation distance, as $k \rightarrow 1$. In fact the same is true at all points along $\Gamma_{\text{Higgs}}(k)$, in this limit: this can be deduced from 4.7. In the light of 2.1, elementary arguments yield:

Theorem 7.1 *As $k \rightarrow 1$, every normal line to the minimal surface, along $\Gamma_{\text{Higgs}}(k)$, becomes exponentially close, relative to separation distance, to a spectral line of the monopole.*

Remark. Of course, this approximation is true anywhere ‘close enough’ to $\Gamma_{\text{Higgs}}(k)$. In general, far away from $\Gamma_{\text{Higgs}}(k)$, the normal lines are not close to spectral lines. Consider, for example, the fact that the maximum distance from the origin, for fixed k , of any spectral line is finite. However, the minimal surface has flat ends and out on these will be normal lines at arbitrary distance from the origin.

Note in particular that the latter observation applies at the two branch points $\pm\beta_2$, on the monopole’s third axis. This is because the branch points on the null curve in \mathbb{C}^3 which engender these move away from \mathbb{R}^3 , as $k \rightarrow 1$.

§8. The Gauss map and curvature concentration.

Recall that the spectral curve of a charge ℓ monopole is an ℓ -fold branched cover of \mathbb{P}_1 in \mathbb{T} . Since the projection map to \mathbb{P}_1 may be identified with the Gauss map, g , of the auxiliary minimal surface determined by osculation, it follows that the monopole energy is:

$$\mathcal{E}(\nabla, \Phi) = 4\pi \deg(g) = 4\pi\ell.$$

Our purpose here is to interpret this global coincidence ‘locally’, when $\ell = 2$. Let \mathcal{K} denote the Gaussian curvature of the branched metric ds^2 on $\mathbb{C}/(\mathbb{Z}\omega_1 + \mathbb{Z}\omega_2)$ induced by the branched minimal immersion. Recall that

$$\int_{\mathbb{C}/(\mathbb{Z}\omega_1 + \mathbb{Z}\omega_2)} \mathcal{K} ds^2 = - \int_{\mathbb{C}/(\mathbb{Z}\omega_1 + \mathbb{Z}\omega_2)} \frac{4|g'|^2}{(1 + |g|^2)^2} dx dy = -4\pi\ell,$$

cf. [13]. The second integral is just the area induced by the Gauss map g : we study the behaviour of

$$G = \frac{4|g'|^2}{(1 + |g|^2)^2},$$

in the limits $k \rightarrow 0, 1$. In particular, we show that it *localises* in these limits. This reflects the behaviour of \mathcal{K} on the surface in \mathbb{R}^3 : as $k \rightarrow 1$, \mathcal{K} localises at the monopole particles. It follows from Theorem 7.1 that in the limit $k \rightarrow 1$, \mathcal{K} measures the twisting of the spectral lines through the particles. The total twisting, measured in the induced metric, equals the monopole’s energy.

Recall that the Gauss map is given by $g(u) = \wp(u) - e_3$. This is related to the Euclidean Gauss map γ , of the minimal surface, via stereographic projection: $\gamma =$

$P^{-1} \circ g$, where $P : S^2 \rightarrow \mathbb{C} \cup \{\infty\}$, $P(x) = (x_1 + ix_2)/(1 + x_3)$. g maps the rectangle with vertices $0, \omega_1/2, \omega_3/2, \omega_2/2$, to the lower half plane so that its boundary maps to \mathbb{R} . Obviously, the behaviour of g on the whole period domain may be inferred from this. The behaviour of the two pairs:

$$\begin{aligned} g(0) &= \infty, & g(\omega_3/2) &= 0, \text{ and} \\ g(\omega_1/2) &= k'/k, & g(\omega_2/2) &= -k/k', \end{aligned}$$

corresponding to the two spectral lines through the origin, elucidates the manner in which g covers \mathbb{P}_1 . In particular, as $k \rightarrow 1$, it appears that G ‘concentrates’ on the quarter-period lines $x = \omega_1/4$, and $x = 3\omega_1/4$. The lines $x = 0$, and $x = \omega_1/2$, map to the circles on S_k that are ‘asymptotically pinched off’, as $k \rightarrow 1$. Moreover, as $k \rightarrow 0$, G appears to ‘concentrate’ on the quarter-period lines $iy = \omega_2/4$, and $iy = 3\omega_2/4$. The lines $iy = 0$, and $iy = \omega_2/2$, map to the circles on S_k that are pinched off at $k = 0$. Despite the simplicity of the expression for g , a deeper insight into these matters is gained through working in monopole coordinates: the symmetries of G with respect to the quarter-period lines, and its behaviour on them are thus revealed.

The Gauss map $\gamma_\Phi : \mathbb{C}/(\mathbb{Z}\omega_1 + \mathbb{Z}\omega_2) \rightarrow Q_1$, with respect to monopole coordinates, is given by differentiating (15)-(17):

$$\gamma_\Phi(u) = [-kf_1(2u), k'f_2(2u), -if_3(2u)].$$

It follows that $g_\Phi : \mathbb{C}/(\mathbb{Z}\omega_1 + \mathbb{Z}\omega_2) \rightarrow \mathbb{C} \cup \{\infty\}$, is given by:

$$g_\Phi(u) = h^{-1} \circ \gamma_\Phi(u) = \frac{-if_3(2u)}{kf_1(2u) + ik'f_2(2u)},$$

where $h : \mathbb{C} \cup \{\infty\} \rightarrow Q_1$, $h(\zeta) = [1 - \zeta^2, i(1 + \zeta^2), -2\zeta]$.

Remark. Let $\gamma_\phi : \mathbb{C}/(\mathbb{Z}\omega_1 + \mathbb{Z}\omega_2) \rightarrow S^2$, be the Euclidean Gauss map of the minimal surface $\phi = \text{Re}(\Phi)$. Observe that g_Φ agrees with γ_ϕ , after the latter is composed with stereographic projection from $-\underline{e}_3$ to the $(\underline{e}_1, \underline{e}_2)$ -plane in \mathbb{R}^3 .

Proposition 8.1(i)

$$g_\Phi(u) = -\frac{k'f_2(2u) + ikf_1(2u)}{f_3(2u)}.$$

(ii)

$$g'_\Phi(u) = \frac{2ig_\Phi(u)}{f_3(2u)}.$$

Proof. (i) follows immediately from $k^2f_1^2 + k'^2f_2^2 - f_3^2 = 0$.

(ii)

$$g'_\Phi(u) = -\left(\frac{\phi'}{f_3} (f_3^2(k'f_2^{-1} + ikf_1^{-1}) - (k'f_2 + ikf_1))\right)(2u),$$

and hence $f_3^2 = (k'f_2 + ikf_1)(k'f_2 - ikf_1)$, implies

$$\begin{aligned} g'_\Phi(u) &= \left(\frac{\wp'}{f_3^2}(k'^2 + k^2 - 1 + ikk'(f_1^{-1}f_2 - f_1f_2^{-1}))\right)(2u)g_\Phi(u) \\ &= ikk' \left(\frac{\wp'(f_2^2 - f_1^2)}{f_1f_2f_3^2}\right) (2u)g_\Phi(u) \\ &= -i \left(\frac{\wp'}{f_1f_2f_3^2}\right) (2u)g_\Phi(u), \end{aligned}$$

since $e_2 - e_1 = -1/kk'$. Finally recall that $\wp' = -2f_1f_2f_3$. \square

Using the evenness/oddness properties of $f_j(2u)$ at appropriate points, elementary considerations reveal that G enjoys symmetries about $H_{\frac{1}{4}}, H_{\frac{3}{4}}, V_{\frac{1}{4}}$ and $V_{\frac{3}{4}}$:

Proposition 8.2 (i) $G(\frac{\omega_1}{4} - \bar{u}) = G(\frac{\omega_1}{4} + u)$.

(ii) $G(\frac{3\omega_1}{4} - \bar{u}) = G(\frac{3\omega_1}{4} + u)$.

(iii) $G(\frac{\omega_2}{4} + \bar{u}) = G(\frac{\omega_2}{4} + u)$.

(iv) $G(\frac{3\omega_2}{4} + \bar{u}) = G(\frac{3\omega_2}{4} + u)$.

We now show that the integral density of Gaussian curvature concentrates on $V_{\frac{1}{4}} \cup V_{\frac{3}{4}}$, as $k \rightarrow 1$, and on $H_{\frac{1}{4}} \cup H_{\frac{3}{4}}$, as $k \rightarrow 0$. The next result follows immediately from 8.1 and $f_3^2 = (k'f_2 + ikf_1)(k'f_2 - ikf_1)$.

Proposition 8.3

$$G(u) = \frac{4|g'_\Phi(u)|^2}{(1 + |g_\Phi(u)|^2)^2} = \frac{8}{k^2|\wp(2u) - e_1| + k'^2|\wp(2u) - e_2| + |\wp(2u) - e_3|}.$$

It clarifies the exposition at this point to introduce the following reparameterizations. Let $\rho_1 : \mathbb{C} \rightarrow \mathbb{C}$, be given by $\rho_1(z) = \omega_1 z$ and $\rho_2 : \mathbb{C} \rightarrow \mathbb{C}$, be given by $\rho_2(z) = |\omega_2|z$, moreover let $\tau_2 = \omega_2/\omega_1$ and $\tau_1 = \omega_1/|\omega_2|$: ρ_1 induces a biholomorphism $\mathbb{C}/(\mathbb{Z}1 + \mathbb{Z}\tau_2) \rightarrow \mathbb{C}/(\mathbb{Z}\omega_1 + \mathbb{Z}\omega_2)$, and ρ_2 a biholomorphism $\mathbb{C}/(\mathbb{Z}\tau_1 + \mathbb{Z}i) \rightarrow \mathbb{C}/(\mathbb{Z}\omega_1 + \mathbb{Z}\omega_2)$.

Let $V'_a := \{a + iy ; 0 \leq y < \tau_2\}$, and $H'_a := \{x + ia ; 0 \leq x < \tau_1\}$. Moreover, let G_1, G_2 , be the integral densities induced by $\phi \circ \rho_1$, and $\phi \circ \rho_2$, respectively, i.e. $G_j(z) = |\omega_j|^2 G(\omega_j z)$, $j = 1, 2$.

Corollary 8.4 For $u \in V_{\frac{1}{4}} \cup V_{\frac{3}{4}}$,

$$G(u) = \frac{4}{k'^2(\wp(2u) - e_2)}.$$

Hence, $G_1 \rightarrow \infty$, on $V'_{\frac{1}{4}} \cup V'_{\frac{3}{4}}$, as $k \rightarrow 1$.

Proof. For such u , $f_1(2u) \in i\mathbb{R}$, $f_2(2u) \in \mathbb{R}$ and $f_3(2u) \in \mathbb{R}$. Therefore

$$\begin{aligned} G(u) &= \frac{8}{-k^2 f_1(2u)^2 + k'^2 f_2(2u)^2 + f_3(2u)^2} \\ &= \frac{8}{2k'^2 f_2(2u)^2}. \end{aligned}$$

Now observe that for $z \in V'_1 \cup V'_3$,

$$4k^2 K(k)^2 \leq \frac{\omega_1^2}{k'^2 (\wp(2\omega_1 z) - e_2)} \leq 4K(k)^2. \quad \square$$

Similarly, we obtain:

Corollary 8.5 For $u \in H'_1 \cup H'_3$,

$$G(u) = -\frac{4}{k^2 (\wp(2u) - e_1)}.$$

Hence, $G_2(u) \rightarrow \infty$ on $H'_1 \cup H'_3$, as $k \rightarrow 0$.

Corollary 8.6 (i) At the quarter-period points we have:

$$G\left(\frac{\omega_1}{4}\right) = \frac{4k}{k'}, \quad G\left(\frac{\omega_2}{4}\right) = \frac{4k'}{k} \quad \text{and} \quad G\left(\frac{\omega_3}{4}\right) = \frac{4}{kk'}, \quad \text{etc.}$$

(ii) $\omega_3/4$ is a maximum of G , $\omega_1/4$ and $\omega_2/4$ are saddle-points.

Remark. Clearly, the behaviour of G at the other quarter-period points may be deduced from symmetry.

Comparing

$$G_1(z) \leq \frac{8\omega_1^2}{|\wp(2\omega_1 z) - e_1|},$$

it can be shown that for $z \notin V'_1 \cup V'_3$, $G_1(z) \rightarrow 0$, as $k \rightarrow 1$. Similarly, for $z \notin H'_1 \cup H'_3$, $G_2(z) \rightarrow 0$, as $k \rightarrow 0$. This can be seen by inspecting power series.

Remark. As $k \rightarrow 1$, narrower and narrower bands around V'_1 and V'_3 are stretched by the Gauss map to cover almost all of the sphere.

The underlying geometrical behaviour of $\gamma_\phi : \mathbb{C}/(\mathbb{Z}\omega_1 + \mathbb{Z}\omega_2) \rightarrow S^2 \subset \mathbb{R}^3$, elucidates the above results:

Theorem 8.7 (i) As u passes from $\omega_1/4$ to $\omega_1/4 + \omega_2$ along V'_1 , the Gauss map $\gamma_\phi(u)$ winds once around the great circle on S^2 that projects to the e_1 -axis under stereographic projection (from $-e_3$). The analogue holds on V'_3 .

(ii) As u passes from $\omega_2/4$ to $\omega_2/4 + \omega_1$ along $H_{\frac{1}{4}}$, the Gauss map $\gamma_\phi(u)$ winds once around the great circle on S^2 that projects to the \underline{e}_2 -axis under stereographic projection (from $-\underline{e}_3$).

Proof. This follows easily from the behaviour of g_Φ , which is real on $V_{\frac{1}{4}} \cup V_{\frac{3}{4}}$, while purely imaginary on $H_{\frac{1}{4}}$. \square

We spell this out in more detail: Passing from $\omega_1/4$ to $\omega_3/4$, ϕ maps onto the Higgs axis between β_1 and β_3 , while the normal vector turns through 90° . Between $\omega_3/4$ and $\omega_1/4 + \omega_2/2$, ϕ maps back along the line segment, but as part of an intersecting ‘sheet’, see Figure 2. This is reflected by the fact that the Gauss map turns through another 90° , and arrives back at β_2 in the antipodal direction. Now, this is all repeated between $\omega_1/4 + \omega_2/2$ and $\omega_1/4 + \omega_2$, except that the values of the Gauss map are antipodal: $\gamma_\phi(u + \omega_2/2) = \alpha(\gamma_\phi(u))$, along $V_{\frac{1}{4}}$. This reflects the fact that on the upper 1/2-rectangle of the period domain, ϕ maps onto the same surface in \mathbb{R}^3 , but with opposite orientation. Of course, the analogue holds along $V_{\frac{3}{4}}$.

As $k \rightarrow 1$, the length of the line segment between β_1 and β_3 goes to zero, but the Gauss map makes one revolution along it for any $k \in (0, 1)$. Thus as $k \rightarrow 1$, it changes rapidly along the line segment, while as $k \rightarrow 0$, it winds slowly, away from β_3 .

Analogous remarks apply to the behaviour of the Gauss map around $\Gamma_{\text{Star}}(k)$. As $k \rightarrow 0$, $\Gamma_{\text{Star}}(k)$ shrinks to 0, but the Gauss map winds around once on $\Gamma_{\text{Star}}(k)$ for all $k \in (0, 1)$. See Figure 1. As $k \rightarrow 1$, $\Gamma_{\text{Star}}(k)$ becomes very large. (Note that $\gamma_\phi(u + \omega_1/2) = \alpha(\gamma_\phi(u))$, on $H_{\frac{1}{4}}$.)

Notice that the branch points $\pm\beta_3$ play a pivotal role, connecting $\Gamma_{\text{Higgs}}(k)$ to $\Gamma_{\text{Star}}(k)$. Moreover the integral density is large at these points in both limits.

We close this section with some observations about the ‘bare’ curvature \mathcal{K} at β_1 and β_2 . As $k \rightarrow 1$, β_1 accompanies β_3 to infinity along the Higgs axis, while β_2 goes off to infinity along \underline{e}_3 , and $\mathcal{K}(\omega_2/4)$, becomes attenuated. As $k \rightarrow 0$, β_1 and β_2 ‘exchange roles’. More precisely, we have:

Proposition 8.8 (i) *There exist constants $\alpha_1, \alpha_2, \alpha_3 \in \mathbb{R}$, such that as $k \rightarrow 0$,*

$$|\mathcal{K}(\frac{\omega_1}{4} + \frac{h}{2})| \leq \alpha_1 k^5 |h|^{-2} + \alpha_2 k^4 + \alpha_3 k^3 |h|^2 + \mathcal{O}(|h|^4).$$

(ii) *There exist constants $\beta_1, \beta_2, \beta_3 \in \mathbb{R}$, such that as $k \rightarrow 1$,*

$$|\mathcal{K}(\frac{\omega_2}{4} + \frac{h}{2})| \leq \beta_1 k'^5 |h|^{-2} + \beta_2 k'^4 + \beta_3 k'^3 |h|^2 + \mathcal{O}(|h|^4).$$

It is not an optimal statement. The proof follows from inspection of Laurent series.

§9. Scattering.

The above results elucidate the behaviour of the family of minimal surfaces generated by the geodesic C_1 on \mathcal{M}_2^0 , which corresponds to a direct collision between two monopole particles, see [2] for further details. We will discuss the details elsewhere, however, we make two comments:

- Note that the 90° scattering of the monopoles is reflected in the behaviour of this family.
- The family includes a point (at the origin) at $k = 0$. As $k \rightarrow 0$, $\Gamma_{\text{Star}}(k)$ shrinks to zero. This is better understood in terms of the two curves on the null curve in \mathbb{C}^3 which project to $\Gamma_{\text{Star}}(k)$. These shrink to the two points $(\pm i\pi/4, 0, 0)$, (in 0-monopole coordinates) and the Gaussian curvature on the null curve concentrates at these points. Recall that the spectral curve of the axially symmetric monopole gives the two stars of spectral affine null planes through these points. Because $(\pm i\pi/4, 0, 0)$ are not in \mathbb{R}^3 , the corresponding configurations of lines in \mathbb{R}^3 do not converge to the star through the origin, see [19].

Remark. In fact it is likely that many of the results described here should be understood directly in terms of the null curve in \mathbb{C}^3 . Cf. [7], [9], [10], [17] and [18].

§10. Charge 3.

Generically, the spectral curve S , of a charge 3 monopole, is a smooth curve on $\mathcal{C}(Q) \subset \mathbb{P}_3$ of genus 4. It is a canonical curve in \mathbb{P}_3 , has degree 6 and is a complete intersection of $\mathcal{C}(Q)$ with a cubic surface.

The covering map to \mathbb{P}_1 has six branch points. These come in antipodal pairs, interchanged by τ , and the three corresponding spectral lines through the origin in \mathbb{R}^3 are perpendicular to the ends of the auxiliary minimal surface. (In general, the auxiliary minimal surface of the generic charge k monopole has k ends.)

Since S is canonical, the points of hyperosculation are the Weierstrass points on S . The total weight of the Weierstrass points is 60. Each of the six branch points of the covering map has weight 4, leaving 36 of weight 1. S is τ -invariant and hence this gives 18 branch points on the auxiliary minimal surface in \mathbb{R}^3 . $18 = 6 \times 3$, where we group the Weierstrass points in the same fibre. In summary we have:

Proposition 10.1 *The auxiliary minimal surface generated by a generic monopole of charge 3 has three ends, total curvature -12π , and 18 branch points in the metric.*

Of course, this does not take us very far. Perhaps the next step is to consider the questions:

- How does the area measure induced on the spectral curve by the Gauss map relate

to the configuration of Weierstrass points?

- How is this reflected in the behaviour of the branch points and Gaussian curvature on the surface in \mathbb{R}^3 ?

However, perhaps all of this is better understood in terms of the role played by the null curve in the geometry of the monopole's complexification?

Appendix

| Quarter-period Values: g_2, g_3 as in (8). | | | |
|--|---|---|--|
| | $u = \frac{\omega_1}{4}$ | $u = \frac{\omega_2}{4}$ | $u = \frac{\omega_3}{4}$ |
| $\wp(u)$ | $\frac{1 + 3k' + k'^2}{3kk'}$ | $-\frac{1 + 3k + k^2}{3kk'}$ | $\frac{k^2 - k'^2}{3kk'} - i$ |
| $\wp'(u)$ | $-\frac{2(1 + k')}{k\sqrt{kk'}}$ | $-\frac{2i(1 + k)}{k'\sqrt{kk'}}$ | $\frac{2(k' + ik)}{\sqrt{kk'}}$ |
| $\wp''(u)$ | $\frac{4(1 + k')}{k'(1 - k')}$ | $\frac{4(1 + k)}{k(1 - k)}$ | $-8 + \frac{4i(k'^2 - k^2)}{kk'}$ |
| $\wp'''(u)$ | $-\frac{8(1 + 3k' + k'^2)}{k'(1 - k')\sqrt{kk'}}$ | $\frac{8i(1 + 3k + k^2)}{k(1 - k)\sqrt{kk'}}$ | $8 \left(\frac{5k^2 - 1}{k\sqrt{kk'}} - i \frac{5k'^2 - 1}{k'\sqrt{kk'}} \right)$ |

Remarks on the Figures.

These were drawn with Mathematica. It is easy to write a short program using (1)-(3), (7)-(9) and (14). It is instructive to do this and experiment with the parameter values. We show the surfaces near parts of Γ_{S_k} only. One can study larger regions but the pictures become very complex, particularly when k is not close to 0. It is also instructive to plot G and \mathcal{K} for various values of k .

Acknowledgements The author is very grateful to Patrick McCarthy for many helpful conversations. He also thanks Werner Nahm and Paul Sutcliffe for useful conversations. He is indebted to the Mathematics Faculty of the University of Southampton for their generous hospitality and thanks Victor Snaith for his invitation. He also thanks the ICTP, Trieste for their hospitality during February and March of 2002.

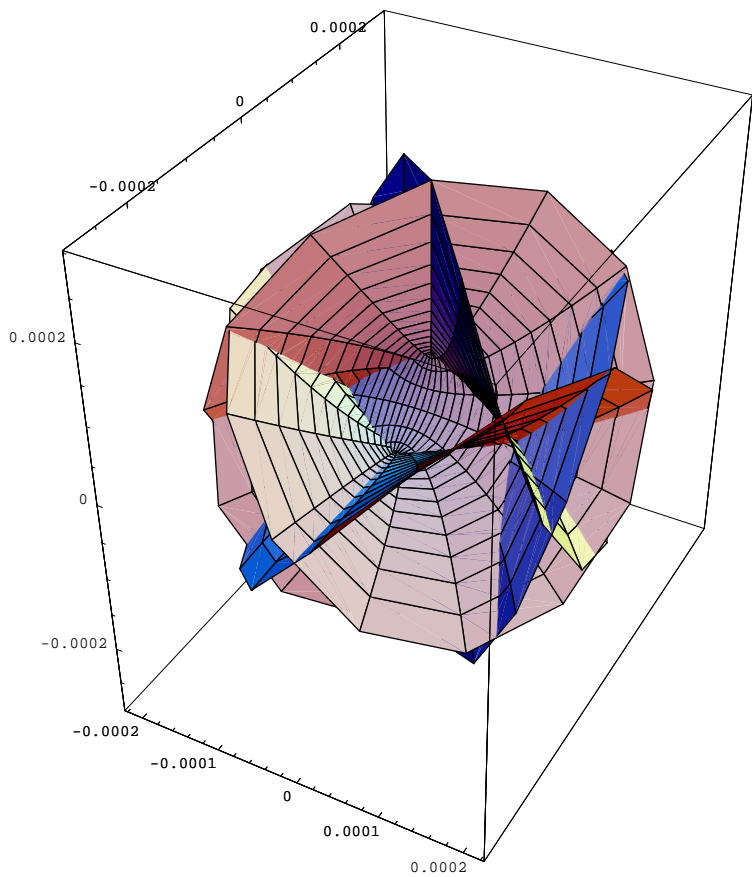


Figure 1: $k = 0.01$, points close to $\Gamma_{\text{Star}}(k)$: $0 \leq x \leq \omega_1$, $\omega_2/4 - 0.05 \leq y \leq \omega_2/4 + 0.05$

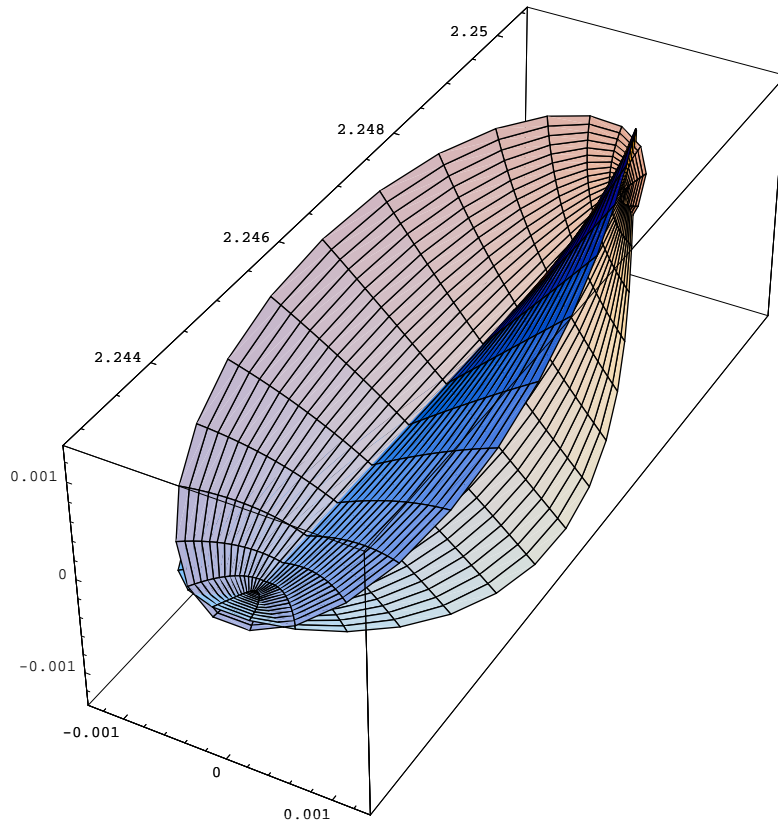


Figure 2: $k = 0.999$, points close to (one half of) $\Gamma_{\text{Higgs}}(k)$: $\omega_1/4 - 0.025 \leq x \leq \omega_1/4 + 0.025$, $0 \leq y \leq \omega_2/2$

References

- [1] M.F. Atiyah, *Solutions of Classical Equations*, Proceedings of 1981 Summer School of Theoretical Physics, Poiana Brasov, Romania, Birkhauser 1982, 207-219.
- [2] M.F. Atiyah and N.J. Hitchin, *The Geometry and Dynamics of Magnetic Monopoles*, Princeton University Press, Princeton 1988.
- [3] G. Darboux, *Lecons sur la Théorie Générale des Surfaces III*, Gauthier-Villars, Paris 1894.
- [4] P. Du Val, *Elliptic Functions and Elliptic Curves*, Cambridge University Press 1973.
- [5] N.J. Hitchin, *Monopoles and Geodesics*, Comm. Math. Phys. 83 (1982), 579-602. Presses De L'Université De Montréal, 1987.
- [6] N.J. Hitchin, N.S. Manton and M.K. Murray, *Symmetric Monopoles*, Nonlinearity 8 (1995), 661-692.
- [7] J. Hurtubise, *Analysis on Manifolds, Some Problems Linking Algebraic and Differential Geometry*, D. Phil. Thesis, Oxford University 1982.
- [8] J. Hurtubise, *SU(2) Monopoles of Charge 2*, Comm. Math. Phys. 92 (1983), 195-202.
- [9] J. Hurtubise, *The Asymptotic Higgs Field of a Monopole*, Comm. Math. Phys. 97 (1985), 381-389.
- [10] J. Hurtubise, *Twistors and the Geometry of Bundles over $\mathbb{P}_2(\mathbb{C})$* , Proc. London Math. Soc. (3) 55 (1987), no. 3, 450-464.
- [11] A. Jaffe and C. Taubes, *Vortices and Monopoles*, Birkhäuser, Boston, 1980.
- [12] L.P. Jorge and W.H. Meeks, *The Topology of Complete Minimal Surfaces of Finite Total Gaussian Curvature*, Topology 22, no.2 (1983), 203-221.
- [13] H.B. Lawson, *Lectures on Minimal Submanifolds, Vol I*, Second Edition, Mathematics Lecture Notes Series 9, Publish or Perish, Inc., Wilmington, Del., 1980.
- [14] R. Osserman, *Global Properties of Minimal surfaces in E^3 and E^n* , Ann. of Math. 80 (1964), 340-364.
- [15] R. Osserman, *A Survey of Minimal Surfaces*, Dover Publications, Inc., New York, 1986.
- [16] A.J. Small, *Duality for a Class of Minimal Surfaces in \mathbb{R}^{n+1}* , Tohoku Math. J. 51 (1999), 585-601.
- [17] A.J. Small, *Singularity Criteria for (Complexified) BPS Monopoles*, Math. Proc. Camb. Phil. Soc. 129 (2000), 59-71.
- [18] A.J. Small, *Osculation and Singularity of Charge 2 (Complexified) BPS Monopoles*, Int. J. Math. 11, No. 7 (2000), 943-948.
- [19] A.J. Small, *The Spectral Lines of the Charge 2 Axially Symmetric Monopole*, preprint.
- [20] P.M. Sutcliffe, *BPS Monopoles*, Int. Jour. Mod. Phys. A, 12 (1997), 4663-4705.
- [21] R.S. Ward and R.O. Wells, *Twistor Geometry and Field Theory*, Cambridge University Press, 1990.